

TRACK SETTling CONTROL OF TRIPLE-STAGE HDD USING
ROBUST OUTPUT FEEDBACK MPC

By

Huy Minh Nguyen

A report submitted in partial satisfaction of the

requirements for the degree of

Masters of Science, Plan II

in

Mechanical Engineering

at the

University of California, Berkeley

Committee in charge:

Professor Roberto Horowitz, Chair

Professor Andrew Packard

Fall Semester 2016

Abstract

Track Settling Control of Triple-Stage HDD using Robust Output Feedback MPC

by

Huy Minh Nguyen

Master of Science in Mechanical Engineering

University of California, Berkeley

Professor Roberto Horowitz, Chair

Track settling control for a hard disk drive with three actuators has been considered. The objective is to settle the read/write head on a specific track by following the minimum jerk trajectory. Robust output feedback model predictive control methodology has been utilized for the control design which can satisfy actuator constraints in the presence of noises and disturbances in the system. The controller is designed based on a low order model of the system and has been applied to a higher order plant in order to consider the case of model mismatch at high frequencies. Since the settling control problem generally requires a relatively low frequency control input, simulation results shows that the head can be settled on the desired track with 10 percent of track pitch accuracy while satisfying actuator constraints. Additionally, when comparing the simulation results with that of an equivalent dual-stage system, the addition of the third stage exhibit increased fine tuning and decreased positioning error at the end of track settling.

Acknowledgments

A special thanks to all of my colleagues at the Computer Mechanical Laboratory at UC Berkeley for all of their support and encouragement in this project.

A special thanks to Roberto Horowitz for accepting me to this project, as well as for all of the guidance and encouragement that he has given me.

Many thanks to Omid Bagherieh for his support, guidance, and feedback through this research, as well as in presentations and paper.

Lastly, I would like to thank, Jinwen Pan for his assistance in providing his models and constraints for working with this project.

Contents

1	Introduction	1
1.1	Background	1
1.2	Motivation	1
1.3	Objectives	2
2	Modeling	3
2.1	Plant Model	3
2.2	Reduced-Order Model	3
2.3	Constraints of The Triple-Stage System	6
2.4	Reference Trajectory	6
3	Controller Design	8
3.1	Robust Output MPC Methodology	8
3.2	Track Settling Control for the Triple-Stage System	10
3.2.1	Control Block Diagram	11
3.2.2	Output Constraints to State Constraints	11
3.3	Controller Initialization	12
3.3.1	Initializing the Observer	12
3.3.2	Initializing the Trajectory and Tracking	13
4	Simulation Results	15
4.1	Simulation and Controller Setup	15
4.2	Results and Discussion	16
4.3	Comparison to Dual-Stage System	20
5	Conclusion	22

List of Figures

2.1	Bode magnitude plots for individual actuators of a triple-stage system	5
3.1	Triple-stage track settling control design, where VCM , PZT , and Th denote the inputs, disturbances, outputs, and actuators of the VCM , PZT , and Thermal actuators respectively.	11
4.1	Actual plant and estimated output results of the robust output feedback MPC controller in tracking the minimum jerk trajectory.	16
4.2	Individual input results for each actuator as calculated by the robust output feedback MPC controller.	17
4.3	Individual output results of each actuator as estimated by the robust output feedback MPC controller and produced by the actual plant.	19
4.4	Magnitude in reference tracking error of triple and dual-stage simulation results.	20

List of Tables

2.1	Limitations considered upon the triple-stage system, and its disturbances for controller design and simulations.	6
4.1	Magnitude in reference tracking error of triple and dual-stage simulation during the last millisecond of the track settling simulations. . . .	21

Chapter 1

Introduction

1.1 Background

Significant amount of data storage during the last decade has increased hard disk drive aerial density. Having a disk with more aerial density requires a more precise control strategy to position the read/write head on specific data track[1–6]. This precise positioning can be achieved by improving the control strategy[7] or introducing more actuators to the system. The current state of the art in HDD industry is the dual-stage control system[8–10] which has voice coil motor (*VCM*) and mili actuator (*PZT*) as actuators. However, there have been several researches on introducing a third actuator to the system which can improve the precision positioning[11–13]. This third actuator in called a micro-actuator and is considered to be a Thermal actuator in this paper.

There are three different scenarios for controlling the read/write head of a HDD[1, 14]: a) seek control b) settling control c) track following control. Consider the scenario in which the read/write head should move from an initial track to a desired track. The seek controller will bring the head to the neighborhood of the desired track, then the settling control tries to settle the head on the desired track. Finally, the track following control will keep the head on the desired track.

1.2 Motivation

In this paper, settling control of a triple-stage system has been studied. The problem of settling control has been previously studied for dual-stage systems using frequency loop shaping control design method[1]. However, this methodology cannot guarantee satisfaction of actuator constraints such as input voltage and stroke limitations. Therefore, model predictive control (*MPC*) is considered for its ability to account for input and output constraints on the system, as well as its ability to iteratively account for and correct deviations between predicted and actual plant outputs. However, two

important issues that arise from using classical *MPC* is that it is not robust and that it usually requires knowledge of the states of the plant. These two problems are limiting the usage of classical *MPC* for triple-stage systems. Because the actuators may receive noise and disturbances due to windage, and also all the states are not directly measurable and only head position can be measured.

To resolve these issues, a method of robust output feedback model predictive control outlined in [15–17] is applied to the triple-stage system to account for the effects of noise and disturbances, as well as to utilize estimated states in lieu of the actual states of the plant. Furthermore, the resulting robust output feedback *MPC* for the triple-stage system is applied to the problem of track settling utilizing the reference trajectory formulation method in [1] in order guide the triple-stage system on a minimum jerk trajectory and achieve settling control to a specific track.

1.3 Objectives

In summary, the main objectives of the controller based on robust output feedback *MPC* are as follows:

- To achieve track settling within a margin of error of at most 10 percent by the end of the settling period.
- Ensure that the input and output constraints of each actuator in the triple stage system are upheld and never violated.
- For the track settling problem to be solved by the generation and tracking of a minimum jerk trajectory

Chapter 2

Modeling

A triple-stage system is composed of a voice coil motor (*VCM*) as a first stage actuator, a piezo-electric transducer (*PZT*) as a second stage actuator, and a Thermal actuator as a third stage actuator. In this section, the plant model for a triple-stage system is introduced. Moreover, the read/write head mounted at the tip of this triple-stage system should follow a reference trajectory in order to settle on a desired track. The procedure for generating this reference trajectory is explained at the end of this section.

2.1 Plant Model

A linear time-invariant steady-state model is derived from the frequency response data of each actuator[11] at $100kHz$ sampling frequency. The obtained plant model represents a 4^{th} order approximation of the *VCM* actuator, a 2^{nd} order approximation of the *PZT* actuator, and a 6^{th} order approximation of the Thermal actuator, which are shown with blue dotted line in Fig. 2.1, obtained from [18]. Combining these steady-state models of the individual stages of the system, we obtain a 12^{th} order causal and discrete steady-state model for the complete plant:

$$x_P^+ = A_P x_P + B_P u + B_P d \quad y = C_P x_P + v \quad (2.1)$$

where A_P , B_P , and C_P denote the steady-state matrices of the plant model, d denotes the input disturbance due to windage, and v denotes the output feedback noise of the plant.

2.2 Reduced-Order Model

Additionally, a reduced-order model is considered in the controller design. Similarly to the plant model, this reduced-order model is derived from the frequency response

data of each actuator[11]. However, the reduced order model is comprised of a 2^{nd} order approximation of the *VCM* actuator, a 2^{nd} order approximation of the *PZT* actuator, and a 1^{st} order approximation of the Thermal actuator, based on [18] and in which the lower frequency gain characteristics of each actuator, including the initial resonance frequencies of the *VCM* and *PZT* actuators are preserved. These reduced order models are shown with green dotted lines in Fig. 2.1. Combining these steady-state models of the individual stages of the system, we obtain a 5^{th} order causal and discrete steady-state model, denoted by the causal steady-state matrices: A , B , and C .

Additionally, the reduced-order model, used in the controller design, represents an approximation of the plant model, and introduces the scenario in which the actual triple-stage system, represented by the plant model, is not completely known to the controller, but an estimated model is available. Fig. 2.1 shows a Bode magnitude plot exhibiting a comparison of the frequency response data, plant models, and reduced-order models for each actuator.

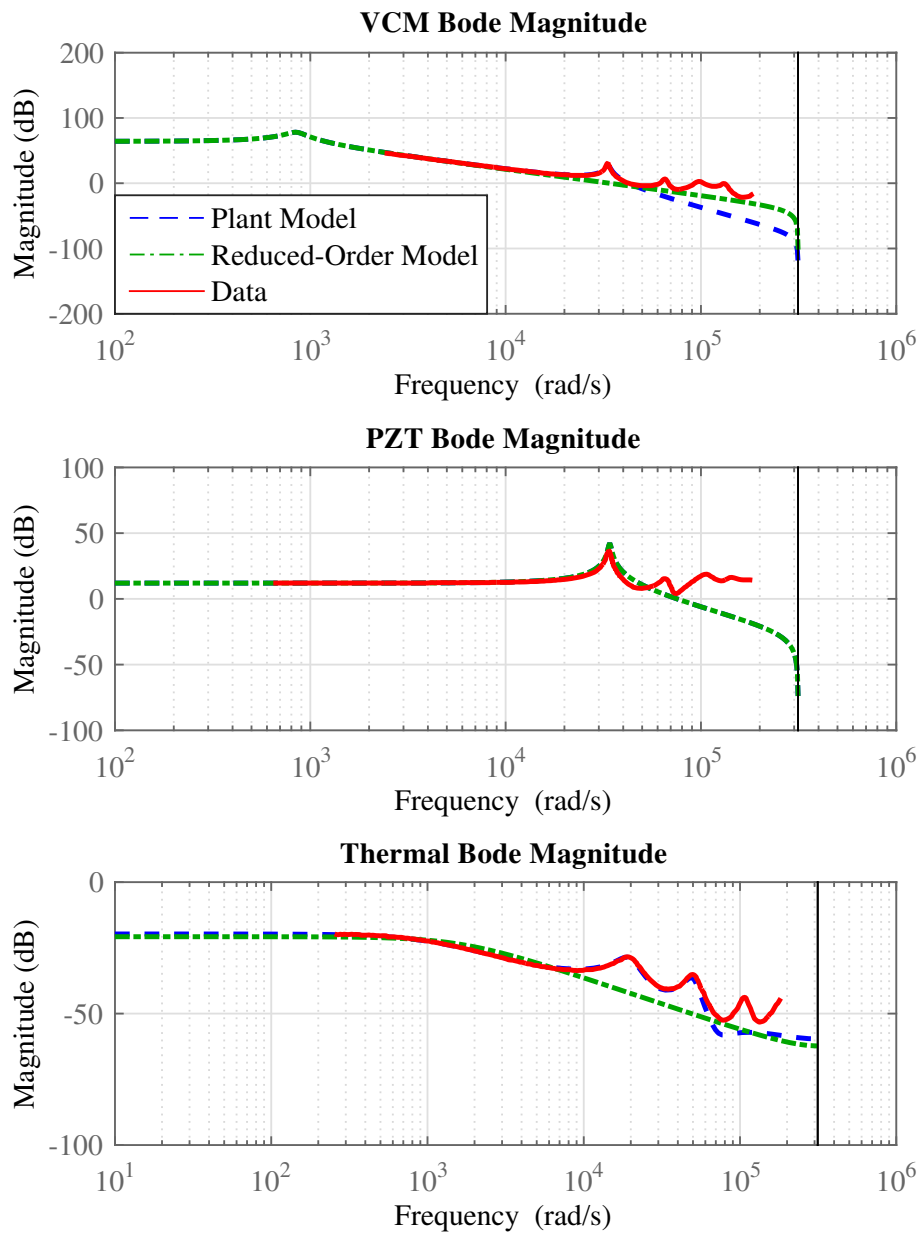


Figure 2.1: Bode magnitude plots for individual actuators of a triple-stage system

2.3 Constraints of The Triple-Stage System

Moreover, constraints on actuator inputs, outputs, noises, and disturbances are also taken into account in the controller design process. According to [11] and [18], limitations of actuator strokes, control input voltages, and disturbances due to windage, of each actuator are listed in Table 2.1 and are used in the design and simulation of the controller and triple-stage system.

Actuators	Actuator Stroke (TP)	Control Input (V)	Input Disturbance (V)
VCM	-	10	1e-4
PZT	6.3	10	1e-5
Th	1.6	20	1e-4

Table 2.1: Limitations considered upon the triple-stage system, and its disturbances for controller design and simulations.

Additionally, measurement noise in the triple-stage system of upto $8e-3 TP$ was considered in the controller design and simulations. In controller and plant simulations, white measurement noise and disturbances were considered to test the controller.

2.4 Reference Trajectory

In the problem of track settling, it is desired to settle to a specific track from a different initial track position. In hard disk drive industry, the head should settle on a desired track by following a minimum jerk trajectory[1]. The minimum jerk trajectory given initial position p_0 , velocity v_0 and acceleration a_0 is given as:

$$\begin{aligned}
 r(k) = & \frac{T_f^2}{2} \left[-\left(\frac{T_s}{T_f}k\right)^5 + 3\left(\frac{T_s}{T_f}k\right)^4 - 3\left(\frac{T_s}{T_f}k\right)^3 + \left(\frac{T_s}{T_f}k\right)^2 \right] a_0 \\
 & + T_f \left[-3\left(\frac{T_s}{T_f}k\right)^5 + 8\left(\frac{T_s}{T_f}k\right)^4 - 6\left(\frac{T_s}{T_f}k\right)^3 + \left(\frac{T_s}{T_f}k\right) \right] v_0 \\
 & + \left[-6\left(\frac{T_s}{T_f}k\right)^5 + 15\left(\frac{T_s}{T_f}k\right)^4 - 10\left(\frac{T_s}{T_f}k\right)^3 + 1 \right] p_0
 \end{aligned} \tag{2.2}$$

where T_f denotes the desired settling period, T_s is the sampling time, k is the iteration number, and $r(k)$ represents the minimum jerk trajectory.

The initial position, p_0 , may be obtained directly from PES measurement. However, v_0 and a_0 must be estimated utilizing previous values of the PES signal, as

well as actuator inputs. These signals have been processed through finite-impulse-response (*FIR*) filters in order to estimate v_0 and a_0 [1]. In order to estimate v_0 , *PES* signal has been processed through a second order derivative filter:

$$F_v(z) = \frac{1.25 - 1.5z^{-1} + 0.25z^{-2}}{T_s} \quad (2.3)$$

Initial acceleration, a_0 has been estimated by passing the input of the *VCM* actuator through the filter:

$$F_a(z) = K_{VCM} \frac{z^{-1} + z^{-2}}{2} \quad (2.4)$$

where K_{VCM} is the gain of *VCM* actuator transfer function.

Chapter 3

Controller Design

In this section, the control strategy behind robust output feedback *MPC* is introduced first[15]. Then, this methodology has been applied to the settling control of a triple-stage hard disk drive. The controller has been designed based on a low order plant but implemented on a higher order plants. Also, the initialization procedure for controller parameters has been presented at the end of this section.

3.1 Robust Output MPC Methodology

In the design of the controller for the triple-stage system, the method of *MPC* is considered for its ability to account for constraints on the inputs and states of the system, as well as its ability to iteratively correct for deviations in expected and actual system outputs. However, two issues that arise are that *MPC* is not robust, which may result in violations of these constraints, and that it usually requires knowledge of the states of the plant. In order to resolve these issues, a robust output feedback methodology outlined in [15] is considered in the design of the controller.

This paper first considers a linear, time-invariant system:

$$x^+ = Ax + Bu + w, \quad y = Cx + v \quad (3.1)$$

that is both controllable and observable and which is subject to unknown, but bounded output noise and input disturbances, v and w which lie within the sets \mathbb{V} and \mathbb{W} . Additionally, the system is also subject to the hard state and input constraints in which x and u must lie within the sets \mathbb{X} and \mathbb{U} , respectively.

Meanwhile, a Luenberger observer is used to estimate the actual states of the system from output feedback:

$$\hat{x}^+ = A\hat{x} + Bu + L(y - \hat{y}), \quad \hat{y} = C\hat{x} \quad (3.2)$$

where L is chosen to ensure that the eigenvalues of $(A - LC)$ lie within the unit circle of the complex plane, and whereby the state estimation error is $\tilde{x} \triangleq x - \hat{x}$.

Furthermore, the *MPC* generates its predictive optimal inputs utilizing the nominal model and state:

$$\bar{x}^+ = A\bar{x} + B\bar{u}, \quad \bar{y} = C\bar{x} \quad (3.3)$$

whereby the error between the estimated and nominal states is $e = \hat{x} - \bar{x}$. The value of error, e and nominal control input \bar{u} are used to construct control input u :

$$u = \bar{u} + Ke \quad (3.4)$$

where K is chosen to ensure that the eigenvalues of $(A + BK)$ lie within the unit circle of the complex plane.

The minimal Robust Positive Invariant (*mRPI*) sets have been used in order to bound the values of \tilde{x} and e signals. These sets are defined in [16]:

A set Ω is a robust positive invariant set for the system $x^+ = f(x, w)$ and constraint set (\mathbb{X}, \mathbb{W}) if $\Omega \subseteq \mathbb{X}$ and $f(x, w) \in \Omega, \forall w \in \mathbb{W}, \forall x \in \Omega$.

To calculate this set for the state estimation error \tilde{x} in [15], Equation (3.2) is subtracted from Equation (3.1) and rewritten as the resulting difference equation:

$$\tilde{x}^+ = (A - LC)\tilde{x} + \tilde{\delta}, \quad \tilde{\delta} = w - Lv \quad (3.5)$$

where $\tilde{\delta}$ lies within the set $\tilde{\Delta}$ defined by $\tilde{\Delta} \triangleq \mathbb{W} \oplus (-LV)^1$.

Utilizing the method defined in [17] and Equation (3.5), the *mRPI* set, \tilde{S} for \tilde{x} is calculated, which satisfies the following relationship:

$$\tilde{x}(0) \in \tilde{S} \implies \tilde{x}(i) \in \tilde{S} \forall i \geq 0 \quad (3.6)$$

Similarly, the *mRPI* set for the observer and nominal state error may be calculated by subtracting Equation (3.3) from Equation (3.2) and rewriting the resulting difference equation as:

$$e^+ = (A + BK)e + \bar{\delta}, \quad \bar{\delta} = LC\tilde{x} + Lv \quad (3.7)$$

where $\bar{\delta}$ lies within the set $\bar{\Delta}$ defined by $\bar{\Delta} \triangleq LC\tilde{S} \oplus LV$.

¹ \oplus represents Minkowski sum.

Again, applying the method defined in [17], the *mRPI* set, \bar{S} for e may be calculated, in which the following relationship is satisfied:

$$e(0) \in \bar{S} \implies e(i) \in \bar{S} \forall i \geq 0 \quad (3.8)$$

After obtaining the *mRPI* sets, \tilde{S} and \bar{S} , these sets are used to impose stricter constraints on the nominal system given in Equation (3.3). Utilizing the relationship between actual and nominal states and that exhibited in Equation (3.4), the following nominal state and input constraints:

$$\bar{\mathbb{X}} \triangleq \mathbb{X} \ominus S \quad S \triangleq \tilde{S} \oplus \bar{S} \quad \bar{\mathbb{U}} \triangleq \mathbb{U} \ominus K\bar{S}^2 \quad (3.9)$$

may be imposed upon the *MPC*, and ensure that the actual state and input constraint sets \mathbb{X} and \mathbb{U} are satisfied even with the unknown noise and disturbances bounded by the sets \mathbb{V} and \mathbb{W} .

The cost function for the *MPC* problem has been defined:

$$V(\bar{x}, \bar{u}) \triangleq (1/2)\bar{x}'_N P \bar{x}_N + \sum_{i=0}^{N-1} (1/2)[\bar{x}'_i Q \bar{x}_i + \bar{u}'_i R \bar{u}_i] \quad (3.10)$$

where Q , R , and P are the cost matrices of the *MPC* penalizing the states, inputs, and terminal states of the *MPC*, respectively. Furthermore, the initial nominal states are selected to satisfy:

$$\hat{x} \in \bar{x} \oplus \bar{S} \quad (3.11)$$

which can ensure the errors in estimated and nominal states become bounded by \bar{S} from the onset of the *MPC* calculation.

3.2 Track Settling Control for the Triple-Stage System

Now that the methodology of robust output feedback *MPC* outlined in [15] has been introduced, the control methodology may be modified and implemented to the higher-order plant model, exhibited in Equation (2.1).

² \ominus represents Minkowski difference.

3.2.1 Control Block Diagram

In order to account for the case in which the full dynamics of the plant are not completely available and to reduce the computational time of $mRPI$ sets, the 5th order reduced-order model is applied as an approximation of the actual plant model in the calculations of the $mRPI$ sets, where discrepancies due to model mismatch may be attenuated and removed by the MPC 's iterative method. The resulting control and plant block diagram is exhibited in Fig. 3.1,

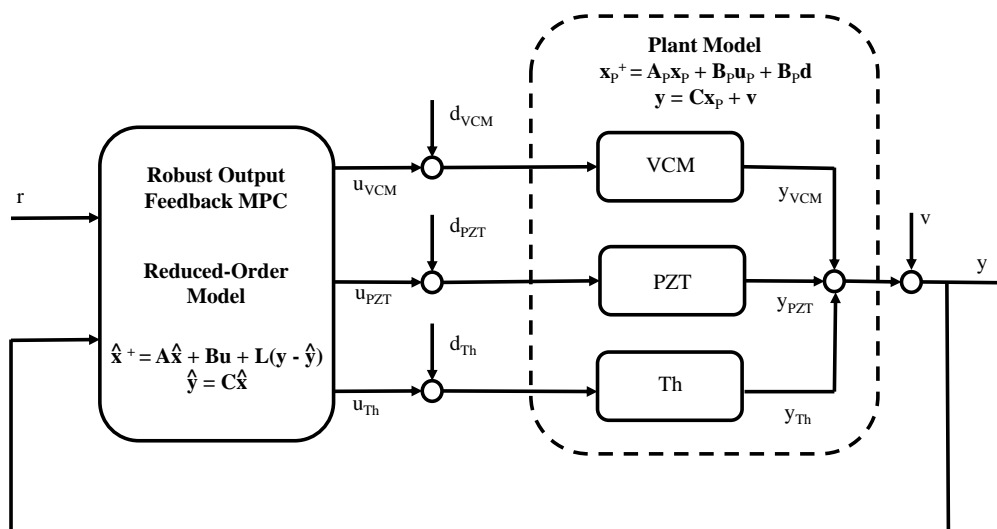


Figure 3.1: Triple-stage track settling control design, where VCM , PZT , and Th denote the inputs, disturbances, outputs, and actuators of the VCM , PZT , and Thermal actuators respectively.

where the MPC calculates optimal inputs for each actuator using the reduced-order model. These inputs are then applied to the higher order plant model to produce the actual outputs of each actuator. The actual outputs are then summed together before being fed back into the MPC along with the reference, r , being tracked.

3.2.2 Output Constraints to State Constraints

Besides the implementation of the plant and reduced-order models, the constraints of the triple-stage system must be taken into account, in the implementation of the triple-stage system. The system input set, \mathbb{U} , and the system state set, \mathbb{X} , may be simply determined using the bounds and constraints provided in [11, 18]. Output of each actuator can be written as:

$$y_{VCM} = C_{VCM}x_{VCM}, \quad y_{PZT} = C_{PZT}x_{PZT}, \quad y_{Th} = C_{Th}x_{Th} \quad (3.12)$$

where the subscripts "VCM", "PZT", and "Th" designate the VCM, PZT, and Thermal actuators respectively. Therefore, the state set \mathbb{X} may be obtained by:

$$\begin{bmatrix} C_{VCM} & 0 & 0 \\ -C_{VCM} & 0 & 0 \\ 0 & C_{PZT} & 0 \\ 0 & -C_{PZT} & 0 \\ 0 & 0 & C_{Th} \\ 0 & 0 & -C_{Th} \end{bmatrix} x \leq \begin{bmatrix} y_{VCM,high} \\ -y_{VCM,low} \\ y_{PZT,high} \\ -y_{PZT,low} \\ y_{Th,high} \\ -y_{Th,low} \end{bmatrix} \quad (3.13)$$

where the subscripts "high" and "low" represent the corresponding upper and lower bounds of the VCM, PZT, and Thermal actuator outputs.

Another issue of importance when implementing the robust output feedback MPC methodology to the triple-stage system is that the disturbance due to windage takes the form of disturbance in the input of the system instead of direct disturbance to the states of the system, shown in Equation (3.1). To resolve this, we reformulate Equation (3.5) as:

$$\tilde{x}^+ = (A - LC)\tilde{x} + \tilde{\delta} \quad \tilde{\delta} = Bd - Lv \quad (3.14)$$

where $\tilde{\delta}$ lies within the set $\tilde{\Delta}$ defined by $\tilde{\Delta} \triangleq B\mathbb{D} \oplus (-LV)$ and input disturbance due to windage satisfies $d \in \mathbb{D}$. Equation (3.14) is then used in place of Equation (3.5) to calculate the *mRPI* set, \tilde{S} .

3.3 Controller Initialization

Since the controller uses a Luenberger observer to estimate the states of the triple-stage system, and the controller does not necessarily have information on the real initial states of the triple-stage system, a method of initializing the controller and the minimum jerk trajectory to which the actuators track must be considered.

3.3.1 Initializing the Observer

In initializing the estimated state of the observer, as the VCM actuator is the only active actuator in track seeking, an estimate of the initial state is made utilizing only the initial, known plant output,

$$\hat{x}_0 = \begin{bmatrix} \frac{y_0}{K_{VCM}} \\ 0 \\ 0 \\ 0 \\ 0 \end{bmatrix} \quad (3.15)$$

Here, the first state is the one controlling the position of the *VC**M* actuator position and K_{VCM} represents the gain on that actuator.

3.3.2 Initializing the Trajectory and Tracking

In order to formulate the minimum jerk trajectory, the initial position, velocity, and acceleration of the output of the triple-stage system must first be determined. To achieve this, the *MPC* controller is allowed to run for a few iterations from its initial state with an initial cost function. In place of the cost function in Equation (3.10), this cost function is defined:

$$\begin{aligned} V(\bar{x}, \bar{u}) \triangleq & (C\bar{x}_N - C\hat{x}_0)'Q(C\bar{x}_N - C\hat{x}_0) \\ & + \sum_{i=0}^{N-1} [(C\bar{x}_i - C\hat{x}_0)'Q(C\bar{x}_i - C\hat{x}_0) + \bar{u}_i'R(k)\bar{u}_i] \end{aligned} \quad (3.16)$$

in which the *MPC* penalizes deviations from the initial position and excessive inputs. $R(k)$ changes with the time step of the system, k , so that the penalization on the inputs of the *PZT* and Thermal actuators decrease over time. As the penalization on the inputs of the *PZT* and Thermal actuators decrease, they gradually become more active in compensating for errors in reference tracking.

After a few iterations of using the cost function in Equation (3.16), the necessary approximations of p_0 , v_0 , and a_0 may be made utilizing Equation (2.3) and Equation (2.4), and the minimum jerk trajectory reference may be formulated using Equation (2.2). The cost function of the *MPC* is switched from Equation (3.16) to the reference tracking cost function:

$$\begin{aligned} V(\bar{x}, \bar{u}) \triangleq & (C\bar{x}_N - r(N + k - j))'Q(C\bar{x}_N - r(N + k - j)) \\ & + \sum_{i=0}^{N-1} [(C\bar{x}_i - r(i + k - j))'Q(C\bar{x}_i - r(i + k - j)) + \bar{u}_i'R(k)\bar{u}_i] \end{aligned} \quad (3.17)$$

where the *MPC* changes from maintaining the initial output, $C\hat{x}_0$, to tracking the reference trajectory, r . Additionally, j represents the step at which minimum jerk

trajectory tracking is initialized.

Furthermore, in order to satisfy Equation (3.11) and track the reference trajectory, the initial nominal states used by the *MPC* at each iteration are selected to satisfy $\hat{x}_k = \bar{x}_0$, as the origin exists in the set \bar{S} .

Chapter 4

Simulation Results

4.1 Simulation and Controller Setup

Prior to track settling, the PZT and Thermal actuators are considered to be at rest, as they are assumed to be inactive during the track seeking phase, prior to track settling.

In the construction of the *mRPI* sets and simulation of the controller, the observer, L , was selected to place the poles of the *VCM* observer at 0.9, whilst leaving those of the *PZT* and Thermal actuators untouched, but within the unit circle of the complex plane. At the same time, the feedback gain K , was chosen so the poles of $(A + BK)$ were placed at $[0.95; 0.9425; 0.9475; 0.945; 0.94]$. Pole placement at these locations prevent the set $K\bar{S}$ in Equation (3.9) from becoming too large and resulting in \bar{U} becoming an empty set.

The discrete sampling frequency used in the *MPC* and simulation was selected as $100kHz$ with k representing the iteration number of the discrete time step of $10\mu s$. The horizon of the *MPC*, N , was selected to be 10 iterations, and the reference trajectory tracking was initialized at the 4th iteration of the *MPC*. The output cost matrix Q was selected to be the identity, whilst $R(k)$ was selected as the following:

$$R(k) = \begin{bmatrix} 1 & 0 & 0 \\ 0 & \alpha_{PZT}(k) & 0 \\ 0 & 0 & \alpha_{Th}(k) \end{bmatrix} \quad (4.1)$$

where the input penalization functions $\alpha_{PZT}(k)$ and $\alpha_{Th}(k)$ are functions that decrease over the time step k . These functions have been adjusted such that the *PZT* and Thermal actuators become increasingly active in reference tracking over time.

where T_{sim} is the length of the simulation, K_{VCM} , K_{PZT} , and K_{Th} are the gains on the transfer functions of the *VCM*, *PZT*, and Thermal actuators respectively.

4.2 Results and Discussion

The triple-stage track settling problem was simulated with our controller using the higher order plant model as discussed in the previous sections. The initial the 12th order plant, x_0 , has been selected as $[-0.84; -0.59; 19; -62; 0; 0; 0; 0; 0; 0; 0; 0]^T$. While the initial states of the 4th order *VCM* actuator correspond to the first four elements of x_0 , the initial states of the 2nd order *PZT* and 6th order Thermal actuator correspond to the following two and six elements of x_0 which have been set at 0. Considering that actuator constraint saturation does not occur for all initial conditions, the initial state of the *VCM* actuator that compose the first four states of x_0 , has been excited and selected such that constraint saturation occurs.

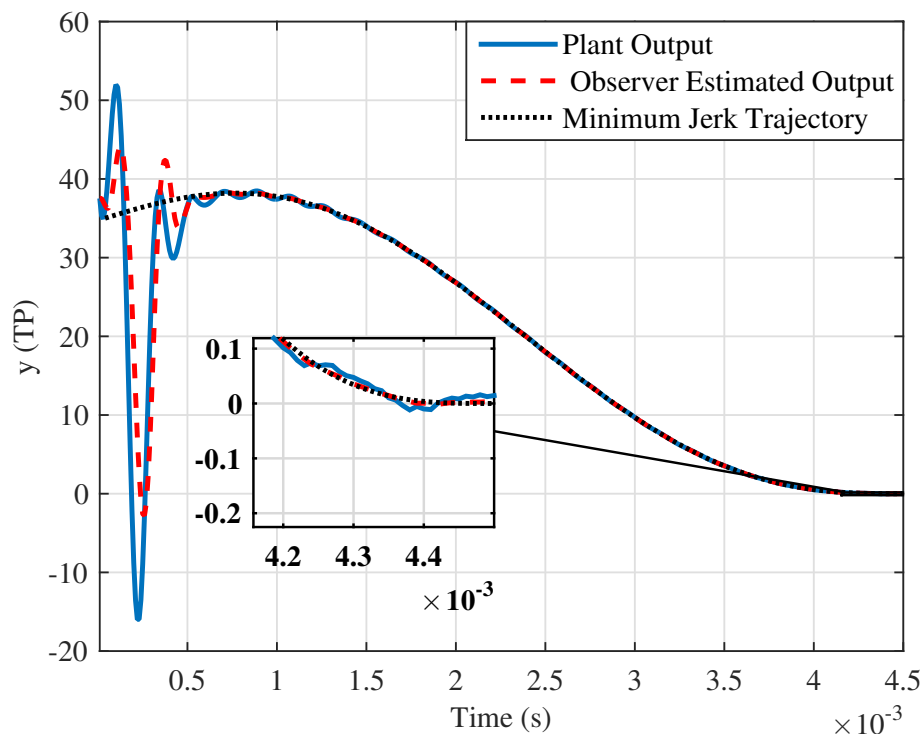


Figure 4.1: Actual plant and estimated output results of the robust output feedback *MPC* controller in tracking the minimum jerk trajectory.

As Fig. 4.1 shows, the robust output feedback *MPC* is capable in guiding the settling of the higher-order plant on the minimum jerk trajectory. Though there is an initial discrepancy in actual and estimated plant outputs, as well as oscillation at the onset of the track settling simulation due to model mismatch and differences in initial estimate and actual plant states, this oscillation quickly decays over time, and the actual and estimated outputs settle onto the desired reference trajectory. By the

end of the settling period, the discrepancy in actual output and reference trajectories are reduced to within a tenth of a track.

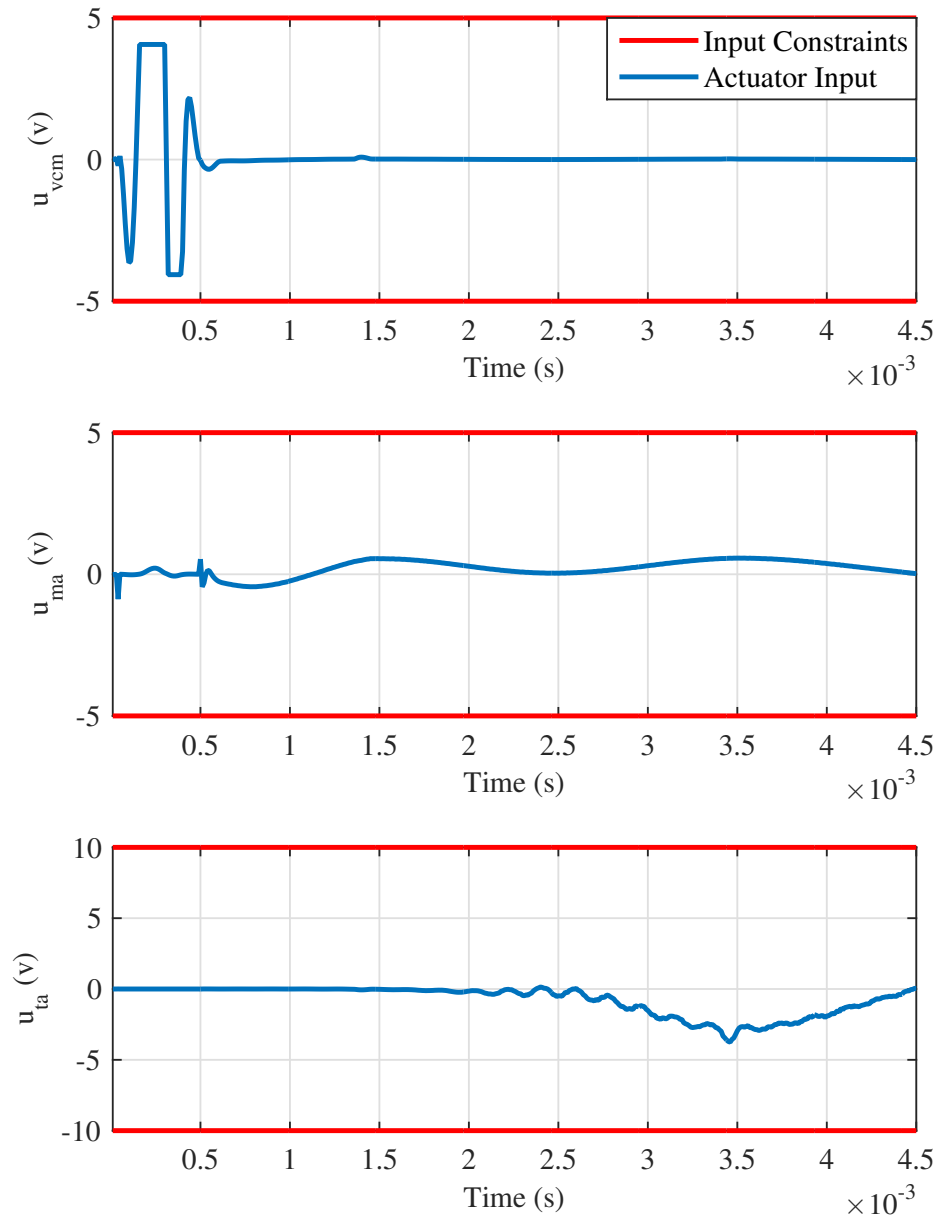


Figure 4.2: Individual input results for each actuator as calculated by the robust output feedback *MPC* controller.

At the same time, as can be viewed in Fig. 4.2, there are no violations of the input constraints of $\pm 5V$, $\pm 5V$, or $\pm 10V$ in either the *VCM*, *PZT*, or Thermal actuators, respectively, even with input disturbance due to windage. Noticeably, in the input of the *VCM* actuator, the input voltage tops off before reaching the *VCM* input constraints of $\pm 5V$. This is due to the stricter constraints, $\bar{\mathbb{U}}$, imposed in the *MPC*, which take into account the worse case scenario of noise and disturbances on the system, to ensure the actual hard constraints, \mathbb{U} are never violated.

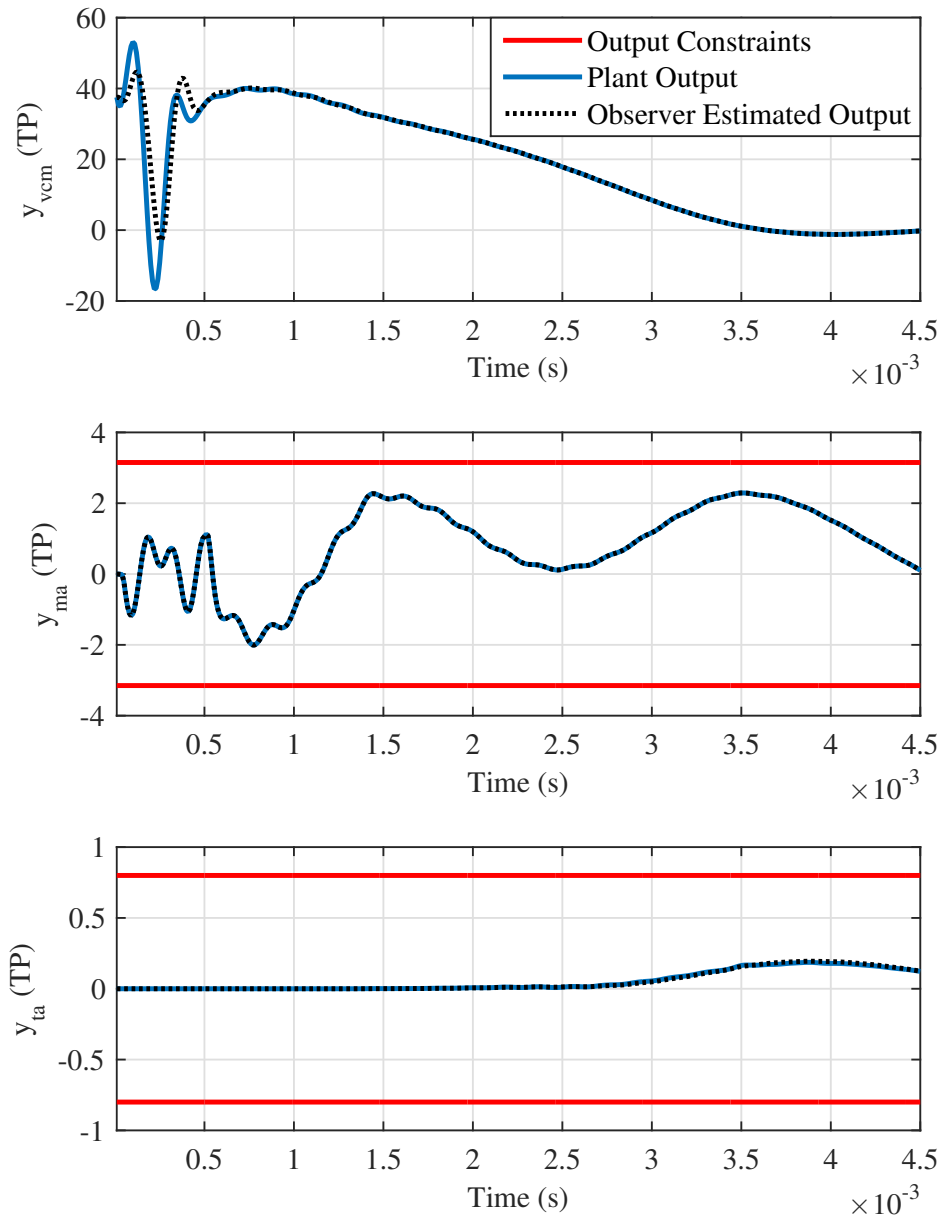


Figure 4.3: Individual output results of each actuator as estimated by the robust output feedback MPC controller and produced by the actual plant.

Similarly, the output constraints of each actuator are satisfied as shown in Fig. 4.3. Here, the *PZT* and Thermal actuators remain within their desired bounds of $\pm 3.15TP$ and $\pm 0.8TP$. As with the inputs to *VCM* actuator, the output of the *PZT* actually

never rises to the actual output constraints of the plant. This is due to the stricter state constraints, $\bar{\mathbf{X}}$, imposed in the *MPC*, which take into account the worst case errors between the actual state and the estimated or nominal states due to noise and disturbances.

Comparing the individual stages of the system in Fig. 4.2 and Fig. 4.3, it can be observed that the *VCM* actuator is naturally most active during the beginning of the track-settling period, when it is used for course positioning of large errors in reference trajectory tracking. In the other case, the *PZT* actuator is used for more moderate positioning during the track settling period, for fixing more minor errors in reference trajectory tracking. Finally, the Thermal actuator becomes active and becomes most important towards the end of the track settling period to compensate for the small discrepancies at the end of the reference trajectory tracking, and for fine position of the head of the triple stage system.

4.3 Comparison to Dual-Stage System

Comparing the results of this triple-stage simulation with that of a dual-stage simulation in which the Thermal actuator remains inactive, Fig. 4.4 exhibits the resulting magnitude in positioning error in tracking the same reference trajectory.

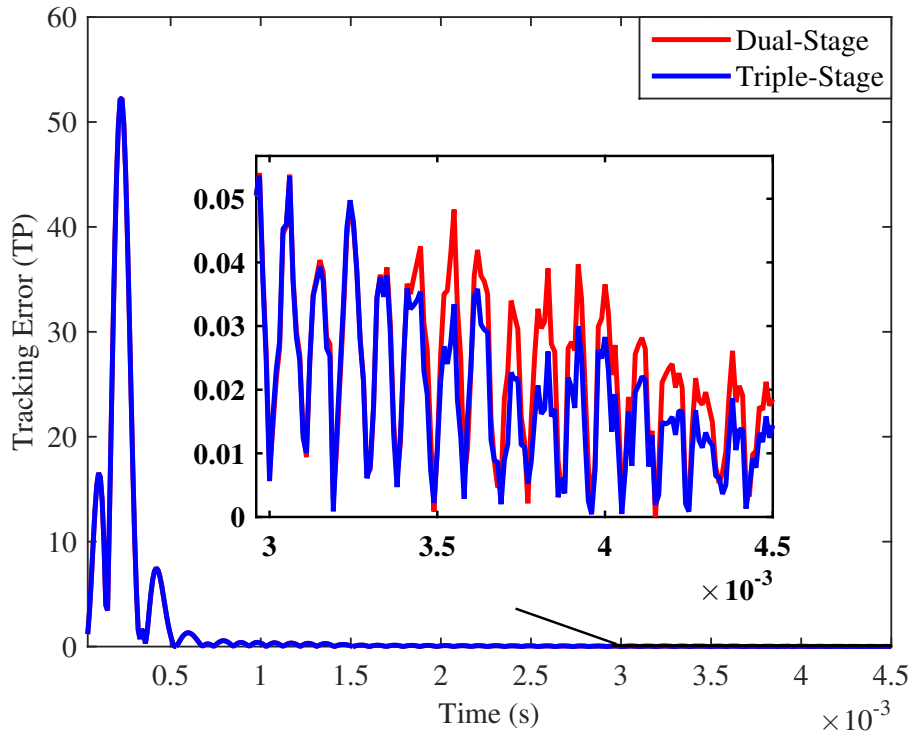


Figure 4.4: Magnitude in reference tracking error of triple and dual-stage simulation results.

Though the two systems remain relatively the same at the beginning of the track settling period, once the Thermal actuator of the triple-stage system becomes active towards the end, the Thermal actuator works to improve reference tracking and reduce tracking error. During the last millisecond of the track settling period, positioning error results of the triple-stage and dual-stage systems are exhibited in Table 4.1.

Configuration	Mean of Error (TP)	Standard Deviation of Error (TP)
Dual-Stage	0.0201	0.0111
Triple Stage	0.0146	0.0084

Table 4.1: Magnitude in reference tracking error of triple and dual-stage simulation during the last millisecond of the track settling simulations.

As can be observed, both the mean and the standard deviation in position error for the triple-stage system are less than that of the equivalent dual-stage system, with a reduction in error of 27.4 percent for the mean and 24.3 percent for the standard deviation.

Chapter 5

Conclusion

In conclusion, the robust output feedback model predictive control method has been applied to track settling problem in a triple-stage system, where the objective is to follow a minimum jerk trajectory. This method has been modified to utilize a low order model, 5th order, for the controller design and applies the designed controller to a higher order plant, 12th order. The designed controller for the triple-stage settling problem has been capable to settle the head on the desired track with 10 percent of track pitch accuracy while satisfying all input and output constraints of the actuators. Moreover, the system has been under the effects of input disturbance due to windage and output noise. An additional comparison of the simulation of the triple-stage settling control to that of a dual-stage system exhibits an improvement in fine position of a 27.4 percent in mean error during the last ms of the track-settling period.

Bibliography

- [1] Hidehiko Numasato and Masayoshi Tomizuka. Settling control and performance of a dual-actuator system for hard disk drives. *Mechatronics, IEEE/ASME Transactions on*, 8(4):431–438, 2003.
- [2] Shiyong Zhou and Masayoshi Tomizuka. Vibration suppression based on adaptive feedforward control with infinite impulse response filter. In *ASME 2015 Dynamic Systems and Control Conference*, pages V003T52A001–V003T52A001. American Society of Mechanical Engineers, 2015.
- [3] Behrooz Shahsavari, Richard Conway, Ehsan Keikha, and Roberto Horowitz. Limits of performance in systems with periodic irregular sampling and actuation rates. In *Proc. of 6th IFAC Symposium on Mechatronic Systems, Hangzhou, China*, 2013.
- [4] Omid Bagherieh, Behrooz Shahsavari, and Roberto Horowitz. Online identification of system uncertainties using coprime factorizations with application to hard disk drives. In *ASME 2015 Dynamic Systems and Control Conference*, pages V002T23A006–V002T23A006. American Society of Mechanical Engineers, 2015.
- [5] Minghui Zheng, Xu Chen, Haiming Wang, Young-Hoon Kim, Wei Xi, and Kuang-Yang Tu. Data storage device comprising slew rate anti-windup compensation for microactuator, April 14 2015. US Patent 9,007,714.
- [6] Omid Bagherieh, Behrooz Shahsavari, Ehsan Keikha, and Roberto Horowitz. Observer design for non-uniform sampled systems using gain-scheduling. In *ASME 2014 Conference on Information Storage and Processing Systems*, pages V001T03A004–V001T03A004. American Society of Mechanical Engineers, 2014.
- [7] Jing Shu Wang, Li Ting Sun, Ming Chi Feng, and Chang An Zhu. Modeling and validation of ultra precision positioning system. In *Applied Mechanics and Materials*, volume 87, pages 200–205. Trans Tech Publ, 2011.
- [8] Daniel Hernandez, Sung-Su Park, Roberto Horowitz, and Andrew K Packard. Dual-stage track-following servo design for hard disk drives. In *American Control*

- Conference, 1999. Proceedings of the 1999*, volume 6, pages 4116–4121. IEEE, 1999.
- [9] T Semba, Takuichi Hirano, J Hong, and L-S Fan. Dual-stage servo controller for hdd using mems actuator. In *Magnetics Conference, 1999. Digest of INTERMAG 99. 1999 IEEE International*, pages DC09–DC09. IEEE, 1999.
- [10] Jianbin Nie and Roberto Horowitz. Design and implementation of dual-stage track-following control for hard disk drives. In *Proceedings of ASME 2nd Dynamic Systems and Control Conference, Hollywood, CA, Oct*, pages 12–14, 2009.
- [11] Chunling Du, Cheng Peng Tan, and Jiaping Yang. Three-stage control for high servo bandwidth and small skew actuation. *Magnetics, IEEE Transactions on*, 51(1):1–7, 2015.
- [12] Takenori Atsumi, Shigenari Nakamura, Masaru Furukawa, Irizo Naniwa, and Jie Xu. Triple-stage-actuator system of head-positioning control in hard disk drives. *Magnetics, IEEE Transactions on*, 49(6):2738–2743, 2013.
- [13] Takenori Atsumi, Shigeo Nakamura, Masaki Odai, Irizo Naniwa, and Shuya Nosaki. Experimental evaluation of triple-stage-actuator system with thermal actuator for hard disk drives. *Journal of Advanced Mechanical Design, Systems, and Manufacturing*, 7(4):722–735, 2013.
- [14] Ben M Chen, Tong Heng Lee, Kemao Peng, and Venkatakrisnan Venkataramanan. *Hard disk drive servo systems*. Springer Science & Business Media, 2006.
- [15] David Q Mayne, SV Raković, Rolf Findeisen, and Frank Allgöwer. Robust output feedback model predictive control of constrained linear systems. *Automatica*, 42(7):1217–1222, 2006.
- [16] Franco Blanchini. Survey paper: Set invariance in control. *Automatica (Journal of IFAC)*, 35(11):1747–1767, 1999.
- [17] SV Raković, Eric C Kerrigan, Konstantinos I Kouramas, and David Q Mayne. Invariant approximations of the minimal robust positively invariant set. *Automatic Control, IEEE Transactions on*, 50(3):406–410, 2005.
- [18] Jinwen Pan, Omid Bagherieh, Behrooz Shahsavari, and Roberto Horowitz. Triple stage track-following servo design for hard disk drives. In *ASME 2016 Dynamic Systems and Control Conference*. American Society of Mechanical Engineers, 2016.